

Biaxial spin-nematic phase of two dimensional disordered rotor models and spin-one bosons in optical lattices

Jean-Sébastien Bernier,¹ K. Sengupta,² and Yong Baek Kim^{1,3}

¹*Department of Physics, University of Toronto, Toronto, Ontario, Canada M5S 1A7*

²*Theoretical Condensed Matter Physics Division, Saha Institute of Nuclear Physics, 1/AF Bidhannagar, Kolkata-700064, India*

³*School of Physics, Korea Institute for Advanced Study, Seoul 130-722, Korea*

(Dated: February 2, 2008)

We show that the ground state of disordered rotor models with quadrupolar interactions can exhibit biaxial nematic ordering in the disorder-averaged sense. We present a mean-field analysis of the model and demonstrate that the biaxial phase is stable against small quantum fluctuations. We point out the possibility of experimental realization of such rotor models using ultracold spin-one Bose atoms in a spin-dependent and disordered optical lattice in the limit of a large number of atoms per site and also suggest an imaging experiment to detect the biaxial nematicity in such systems.

PACS numbers: 75.10.Nr, 71.35.Lk, 03.75.Mn

I. INTRODUCTION

Nematic phases of matter have been widely studied in many different areas of condensed matter physics¹. For example, consider a system of molecules having some vector quantity (say a polarization vector \mathbf{p}) associated with each of them. Since molecules are extended objects, a local coordinate system can be attached to each molecule. Hence, for a molecule at a point i , one can define a local nematic order parameter: $Q_i^{\alpha\beta} = p_{i\alpha}p_{i\beta} - \sum_{\alpha} p_{i\alpha}^2/3$ ¹. The nematic phase is then defined as the state of the system for which $\sum_i \mathbf{p}_i = 0$ whereas $\sum_i Q_i^{\alpha\beta}$ becomes a traceless 3×3 matrix with eigenvalues $Q = [-(Q_1 + Q_2), Q_1, Q_2]$. Such phases are of two types: uniaxial nematic where $Q_1 = Q_2$ and biaxial nematic for which $Q_1 \neq Q_2$ ¹. In both these phases, the system breaks rotational symmetries while preserving translational invariance. Uniaxial nematic phases occurs more frequently whereas the first experimental observation of biaxial nematic phase in a classical system of molecules has only been recently reported². Although much more difficult to realize, biaxial nematic phases are of great theoretical interest since they are known to support non-Abelian defects³. Uniaxial nematic phases have also been studied in the context of several quantum condensed matter systems such as strongly correlated electron systems^{4,5,6,7,8,9,10} and ultracold spin-one atoms in optical lattice^{11,12,13}. For example, in the case of spin-one boson system, in some parameter regime, the ground state breaks spin-rotational invariance along one of the axes while maintaining translational invariance with no spin-order $\langle \mathbf{S} \rangle = 0$ and with two equal non-zero eigenvalues of the matrix $\langle S^\alpha S^\beta \rangle$. However, there has been no proposals of realization of biaxial nematic ground states in the context of quantum condensed matter systems using standard local Hamiltonians.

In this work, we point out that disordered $O(2)$ rotor models with quadrupolar interaction in two dimensions (2D) can exhibit biaxial nematic phase in the disorder averaged sense. Such rotor models are described by the Hamiltonian

$$\mathcal{H}_{\text{rotor}} = U \sum_i L_i^2 - g \sum_{\langle ij \rangle} \left(\sum_{a=x,y,z} d_{ia} \Lambda_{ij}^a d_{ja} \right)^2 \quad (1)$$

where $\mathbf{d} \equiv (d^x, d^y, d^z) = (\sin \theta \cos \phi, \sin \theta \sin \phi, \cos \theta)$ is a unit vector expressed in terms of the rotor angles θ and ϕ , L_i denotes angular momentum of the rotor, $\sum_{\langle ij \rangle}$ denotes sum over nearest neighbor sites, and Λ_{ij} are dimensionless random couplings between the unit vectors \mathbf{d} at sites i and j . In the following we shall consider $\Lambda^x = \Lambda^y \neq \Lambda^z$, and choose $\Lambda^{x(z)}$ to have Gaussian distributions with same width $\delta\Lambda$ and means $\bar{\Lambda}^{x(z)}$. The main result of this work is that in the limit $|\bar{\Lambda}^x - \bar{\Lambda}^z|/\delta\Lambda \ll 1$, the model given by Eq. 1 exhibits a biaxial nematic ground state in the disordered average sense for $U \ll g$. We also show, using a mean-field analysis, that the biaxial phase is stable against quantum fluctuations until $\nu = g/U$ is reduced to a critical value ν_c . Note that the above-mentioned regime can also be reached for arbitrarily weak disorder: $\delta\Lambda \ll \bar{\Lambda}^x, \bar{\Lambda}^z$ provided that $|\bar{\Lambda}^x - \bar{\Lambda}^z| \ll \delta\Lambda$. This particular feature of the rotor model, as we shall see, makes it easily realizable using ultracold atoms in optical lattices.

The choice of the rotor Hamiltonian (Eq. 1) is not arbitrary, but is motivated by their connection with ultracold spin-one bosons in an optical lattice. The low energy effective Hamiltonian of such bosons systems has been derived in the absence of disorder in Refs. 11,12,13. It has been shown that the effective theory of the Mott phases of such a system can be described, in the limit of large number of bosons per site, by rotor models similar to Eq. 1, supplemented by an additional constraint on the number N and the total spin S of the bosons per site: $N + S = \text{even}$ ^{11,12,13}. We generalize this analysis to include disorder and show that in the presence of spin-dependent disordered optical lattices, which can be easily created by using a speckled laser field^{14,15}, the Mott phases of ultracold spin-one bosons is indeed described by Eq. 1 supplemented by the constraint condition mentioned above. Further, as will be shown later, for $U \ll g$, the constraint condition becomes irrelevant and in this limit we expect our analysis of the rotor model to apply for the bosons as well. This correspondence therefore allows us to suggest experiments on ultracold atoms which can in principle probe such a biaxial nematic phase. We suggest a straightforward imaging of ultracold atoms using a polarized laser beam which can distinguish the biaxial phase from other spin or uniaxial nematic phases.

The organization of the paper is as follows. In Sec. II, we analyze the rotor model (Eq. 1) and demonstrate that it exhibits a biaxial nematic ground state. This is followed by Sec. III A, where we derive the effective low-energy Hamiltonian of spin-one ultracold Bosons in a spin-dependent disordered optical lattice and discuss its relation to the rotor model analyzed in Sec. II. In Sec. III B, we suggest an experiment to detect biaxial nematic order. Finally, we conclude in Sec. IV.

II. ANALYSIS OF THE ROTOR MODEL

In this section, we first present an analysis of the rotor model (Eq. 1) and demonstrate the presence of biaxial nematicity at $U = 0$. This is followed by the derivation and analysis of a mean field theory for finite U which illustrates the stability of the biaxial phase against small quantum fluctuations.

A. Limit of $U = 0$

For $U = 0$, in the absence of quantum fluctuations, the Hamiltonian (Eq. 1) is diagonal in the $|\theta, \phi\rangle$ basis. This allows us to write

$$H'_{\text{rotor}} = -g \sum_{\langle ij \rangle} A_{ij}^2, \quad (2)$$

where A_{ij} is given by

$$A_{ij} = \Lambda_{ij}^x \sin \theta_i \sin \theta_j \cos(\phi_i - \phi_j) + \Lambda_{ij}^z \cos \theta_i \cos \theta_j \quad (3)$$

with $0 \leq \theta_i \leq \pi$ and $0 \leq \phi_i < 2\pi$. Let us now consider a ground state configuration of the Hamiltonian H'_{rotor} given by

$$|\Psi_G = |\theta_1^0, \phi_1^0; \theta_2^0, \phi_2^0; \dots; \theta_N^0, \phi_N^0; \dots\rangle \quad (4)$$

where (θ_i^0, ϕ_i^0) denotes the value of the angles θ and ϕ at the i th site in the ground state. From Eqs. 2 and 3, one can immediately see that H'_{rotor} has an infinite number of degenerate ground states since any local transformation $\theta_i^0 \rightarrow \pi - \theta_i^0$, $\phi_i^0 \rightarrow \phi_i^0 + \pi$ leaves H'_{rotor} invariant for any random set of $\Lambda_{ij}^{x,z}$. It is also easy to see that such a local transformation changes $\mathbf{d}_i \rightarrow -\mathbf{d}_i$ and leaves the local nematic order parameter $Q_i^{ab} = d_i^a d_i^b - \delta_{ab}/3$ invariant. Hence for the purpose of computing the nematic order parameter, we can choose any one of these ground state configurations.

The rotor Hamiltonian H'_{rot} is also invariant under two global transformations. The first of them $T_1 : \phi \rightarrow \phi + \eta$ is a gauge freedom which allows us to choose the orientation of the global x axis. The second transformation $T_2 : \theta \rightarrow \pi - \theta$ leaves the diagonal components of Q_{ab}^i invariant while changing the off-diagonal components. The ground states Ψ_G (Eq. 4) and $T_2 \Psi_G = \Psi'_G$ are degenerate.

Using the above-mentioned local and global transformation properties, we can considerably simplify the numerical procedure for obtaining ground states of H'_{rotor} for a given disorder realization. First, from Eq. 3, we find that any ground-state

configuration Ψ_G will always have $\phi_i - \phi_j = 0, \pi$. Using the transformation T_1 , we can therefore choose each individual ϕ_i to be either 0 or π . This is a gauge choice and, hence, does not affect any physical quantity. Next instead of using Ψ_G to compute Q_{ab}^i , we find the state Ψ''_G , for which $\phi_i = 0$ at every site. This can be done since Ψ''_G is always a part of the degenerate states which can be reached from Ψ_G by successive application of the above-mentioned local transformation. Using these two facts, we see that for any set of random coefficients $\Lambda_{ij}^{x,z}$, one can compute $Q_{ab} = \sum_i d_{ia} d_{ib} - \delta_{ab}/3$ by finding the ground state configuration of $H''_{\text{rotor}} = -g \sum_{\langle ij \rangle} (A'_{ij})^2$ with

$$A'_{ij} = \Lambda_{ij}^x \sin \theta_i \sin \theta_j + \Lambda_{ij}^z \cos \theta_i \cos \theta_j. \quad (5)$$

The ground states of H''_{rotor} is two-fold degenerate and these two ground states $\Psi_G^{(1)}$ and $\Psi_G^{(2)} = T_2 \Psi_G^{(1)}$ are related by the global transformation T_2 . The two ground states have opposite signs for off-diagonal elements of Q_{ab} in the chosen gauge and therefore after averaging over these ground states, the off-diagonal elements of Q_{ab} vanishes. Thus we are finally left with the diagonal components $Q_{aa} = -(Q_1 + Q_2)$, $Q_1, Q_2 = (C - 1/3, -1/3, -(C - 2/3))$, where $0 \leq C \leq 1$, for a given set of random coefficients $\Lambda_{ij}^{x,z}$. Finally, one can numerically average over different realizations $\bar{Q}_a = \langle Q_{aa} \rangle_{\text{disorder}}$ to obtain the disorder-averaged nematic order parameter. The biaxial nematic phase is realized when $\bar{C} \neq 0, \frac{1}{2}$ or 1.

The ground state of H''_{rotor} can be obtained numerically using standard minimization procedure for each disorder realization. For the sake of brevity, we choose $\Lambda_{ij}^{x(z)}$ to be a set of random numbers having a Gaussian distribution with same standard deviation $\delta\Lambda$ and different means $\bar{\Lambda}^{x(z)}$ and average over 500 disorder realizations. We choose $\bar{\Lambda}^x > \bar{\Lambda}^z$ here without loss of generality. We study finite-size systems with sizes ranging from $N_S = 8 \times 8$ to $N_S = 20 \times 20$ with periodic boundary conditions and use standard $1/N_S$ extrapolation to obtain the infinite system size limit¹⁶. A few comments about the numerical procedure are in order here.

First, for $(\bar{\Lambda}^x - \bar{\Lambda}^z)/\delta\Lambda \gg 1$, it is clear that the system energy reaches its minimum at $\sin \theta_i \sin \theta_j = 1$ and $\cos \theta_i \cos \theta_j = 0$ for all sites and disorder realizations. Consequently, after disorder-averaging, $\bar{C} = 1$, and the ground state is an uniaxial nematic phase.

Second, in the limit $(\bar{\Lambda}^x - \bar{\Lambda}^z)/\delta\Lambda \ll 1$, for a given disorder realization, we find that the configuration with minimum energy is part of a group of three possible solutions. The first corresponds to $\sin \theta_i \sin \theta_j = 1$ and $\cos \theta_i \cos \theta_j = 0$ for all sites. For a single disorder realization with this solution, the order parameter then has $C = 1$. The second solution possibly assumed by the system is $\sin \theta_i \sin \theta_j = 0$ and $\cos \theta_i \cos \theta_j = \pm 1$ for all sites. The value of the order parameter corresponding to such a disorder realization is then given by $C = 0$. Finally, the third possible solution corresponds to a configuration for which $\sin \theta_i \sin \theta_j$ and $\cos \theta_i \cos \theta_j$ are neither 0 nor ± 1 , and are varying in values from site to site. For such a disorder realization, $C \neq 0, \frac{1}{2}$ or 1 and one has a biaxial

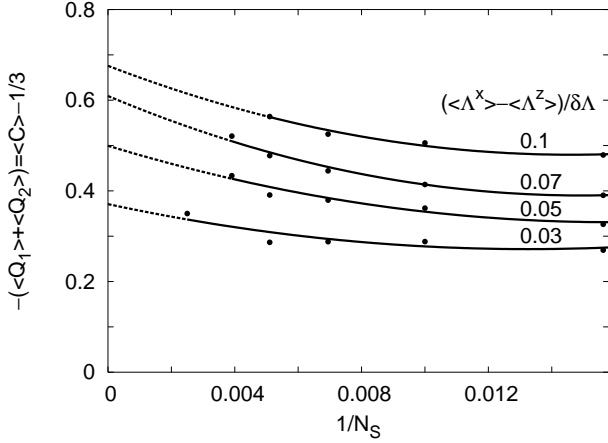


FIG. 1: $-(\bar{Q}_1 + \bar{Q}_2) = \bar{C} - 1/3$ as a function of the inverse lattice size for several disorder strengths. For moderate disorder $(\bar{\Lambda}^x - \bar{\Lambda}^z)/\delta\Lambda \geq 0.1$, an extrapolation to large system size shows that the ground-state will be uniaxially ordered, $\bar{C} \rightarrow 1$. For strong disorder $(\bar{\Lambda}^x - \bar{\Lambda}^z)/\delta\Lambda \leq 0.07$, the ground-state remains biaxially ordered, $\bar{C} \neq 1$ after disorder averaging within $1/N_S$ extrapolation. [Note: $\bar{Q}_1 = \langle Q_1 \rangle$, $\bar{Q}_2 = \langle Q_2 \rangle$, $\bar{C} = \langle C \rangle$, $\bar{\Lambda}^x = \langle \Lambda^x \rangle$, $\bar{\Lambda}^z = \langle \Lambda^z \rangle$]

nematic. However, having $C \neq 0, \frac{1}{2}$ or 1 for a single disorder realization does not guarantee that the system is biaxially ordered. The system can in fact be separated into domains, each domain representing one of the three possible solutions. For example, the system could be separated into domains representing only the first and second type of solutions and still have $C \neq 0, \frac{1}{2}$ or 1. Nonetheless, this situation is unlikely; in most cases where $C \neq 0, \frac{1}{2}$ or 1 we find that the system adopts the third solution. Nevertheless, as mentioned previously, to find the physically meaningful ground state, we need to average over many disorder realizations and by doing so restore the translational invariance of the system. Consequently, $\bar{C} \neq 0, \frac{1}{2}$ or 1 can be used only after disorder-averaging to determine whether the system is biaxially ordered for certain disorder strength.

The result of the numerical calculation, which corroborates the above discussion, is shown in Fig. 1. After fitting second order polynomial functions to our data and extrapolating the resulting functions to $1/N_S \rightarrow 0$, we find that for $(\bar{\Lambda}^x - \bar{\Lambda}^z)/\delta\Lambda \leq 0.07$, the ground state is biaxial nematic with $\bar{C} \neq 1$. For intermediate or larger values of $(\bar{\Lambda}^x - \bar{\Lambda}^z)/\delta\Lambda \geq 0.1$, $\bar{C} = 1$ and we have an uniaxial nematic ground state. So this demonstrates that for $U = 0$, the rotor model exhibits a biaxial nematic ground state in the disordered average sense in the limit $(\bar{\Lambda}^x - \bar{\Lambda}^z)/\delta\Lambda \ll 1$. In the next subsection, we study the effect of quantum fluctuations on this state.

A comment about the validity of the $1/N_S$ extrapolation is in order here. This procedure definitely leaves open a possibility that a large enough system size has not been reached in our numerics and the biaxial nematic state seen here is an artifact of finite system size. The resolution of this question, within our numerical procedure, is not straightforward. However, we can be certain that even if this is the case, with small enough

$(\bar{\Lambda}^x - \bar{\Lambda}^z)/\delta\Lambda$, the biaxial phase will manifest itself over a large window of energy scale at finite temperature, even if the zero temperature ground state turns out to be uniaxial nematic.

B. Quantum fluctuations for $U \neq 0$

To study the effect of quantum fluctuations, it is more convenient to switch to a path integral representation of the rotor Hamiltonian (Eq. 1). To this end, we first write the partition function of our Hamiltonian as

$$Z = \text{Tr} \exp(-\beta \mathcal{H}_{\text{rotor}}) = \text{Tr} \exp[-\beta(T + V)] \quad (6)$$

$$T = U \sum_i L_i^2 \quad (7)$$

$$V = -g \sum_{abcd} \sum_{\langle ij \rangle} d_{ia} d_{jb} \Gamma_{ij}^{abcd} d_{ic} d_{jd} \quad (8)$$

where we have introduced the notation $\Gamma_{ij}^{abcd} = \Lambda_{ij}^a \Lambda_{ij}^c \delta_{ab} \delta_{cd}$. To obtain the partition function we calculate the trace in (6) by writing it as a path integral over M time slices, and then inserting a complete set of coherent states $|\theta, \phi\rangle$ over each slice, so that

$$\begin{aligned} Z &= \lim_{M \rightarrow \infty} \text{Tr} [\exp \{-\delta\tau(T + V)\}]^M \\ &= \int \mathcal{D}\theta \mathcal{D}\phi \prod_{\alpha=0}^{M-1} \langle \theta(\tau_{\alpha+1}); \phi(\tau_{\alpha+1}) | \exp[-\delta\tau T] \\ &\quad \times \exp[-\delta\tau V] | \theta(\tau_\alpha); \phi(\tau_\alpha) \rangle \end{aligned} \quad (9)$$

where $\delta\tau = \beta/M$. Inserting a set of complete states $|l, m\rangle$ (defined by $\langle \theta, \phi | l, m \rangle = Y_{lm}(\theta, \phi)$, where Y_{lm} are the spherical harmonics) on each slice, we get

$$\begin{aligned} Z &= \int \mathcal{D}\theta \mathcal{D}\phi \prod_{\alpha=0}^{M-1} \exp[-\delta\tau V(\theta, \phi)] T_\alpha \quad (10) \\ T_\alpha &= \sum_{l_\alpha=0}^{\infty} \sum_{m_\alpha=-l_\alpha}^{l_\alpha} \prod_i \exp[-U\delta\tau l_\alpha(i) (l_\alpha(i) + 1)] \\ &\quad \times Y_{l_\alpha(i), m_\alpha(i)}^*(\theta_{\alpha+1}(i), \phi_{\alpha+1}(i)) \\ &\quad \times Y_{l_\alpha(i), m_\alpha(i)}(\theta_\alpha(i), \phi_\alpha(i)) \end{aligned} \quad (11)$$

To rewrite (11) in a suitable form, we use the identities¹⁷

$$\begin{aligned} e^{h \cos(\Delta\theta)} &= \sqrt{\frac{8\pi^3}{h}} \sum_{l=0}^{\infty} \sum_{m=-l}^l I_{l+\frac{1}{2}}(h) Y_{lm}^*(\theta, \phi) Y_{lm}(\theta', \phi') \\ \lim_{h \rightarrow \infty} I_{l+\frac{1}{2}}(h) &= \exp\left[-\frac{(l+1/2)^2 - 1/4}{2h}\right] + O(1/h^2) \end{aligned} \quad (12)$$

where $I_{l+\frac{1}{2}}$ is the modified Bessel function and $\cos \Delta\theta = \cos \theta \cos \theta' + \sin \theta \sin \theta' \cos(\phi - \phi')$. Then, after a few straightforward manipulations, we get in terms of $\mathbf{d} =$

($\sin \theta \cos \phi, \sin \theta \sin \phi, \cos \theta$) fields,

$$Z = \int \mathcal{D}\mathbf{d} \prod_i \delta \left(\sum_a |d_{ia}|^2 - 1 \right) \exp(-S) \quad (13)$$

$$S = \int d\tau \left[\sum_{ia} (\partial_\tau d_{ia})^2 - \nu \sum_{\langle ij \rangle} \sum_{abcd} d_{ia} d_{ic} \Gamma_{ij}^{abcd} d_{jb} d_{jd} \right] \quad (14)$$

where we have rescaled $\delta\tau$ so that $4U\delta\tau = 1$ and $\nu = g/4U$.

Next, we introduce a Lagrange multiplier field $\lambda_i(\tau)$ to implement the constraint and decouple the quartic term in S using an auxiliary field N_{ab}^i . After some algebra, we get

$$Z = \int \mathcal{D}\mathbf{d} \mathcal{D}N \mathcal{D}\lambda \exp(-S_1) \quad (15)$$

$$S_1 = \int d\tau \left[\sum_i \left[\sum_a (\partial_\tau d_{ia})^2 + i\lambda_i \left(\sum_a |d_{ia}|^2 - 1 \right) - i \sum_{ab} d_{ia} d_{ib} N_{ab}^i \right] - \frac{1}{2\nu} \sum_{\langle ij \rangle} \sum_{abcd} N_{ac}^i (\Gamma_{ij}^{abcd})^{-1} N_{bd}^j \right] \quad (16)$$

where the auxiliary fields N_{ab}^i are not the order parameter fields, but their conjugate. The order parameter fields P_{ab}^i can now be introduced by a second Hubbard-Stratonovich transformation which yields

$$Z = \int \mathcal{D}\mathbf{d} \mathcal{D}N \mathcal{D}\lambda \mathcal{D}P \exp(-S_{\text{eff}}) \quad (17)$$

$$S_{\text{eff}} = \int d\tau \left[\sum_i \left\{ \sum_a (\partial_\tau d_{ia})^2 + i\lambda_i \left(\sum_a |d_{ia}|^2 - 1 \right) - i \sum_{ab} N_{ab}^i (d_{ia} d_{ib} - P_{ab}^i) \right\} - \nu \sum_{\langle ij \rangle} \sum_{abcd} P_{ac}^i \Gamma_{ij}^{abcd} P_{bd}^j \right] \quad (18)$$

An integration over the auxiliary fields N_{ab}^i shows that $P_{ab}^i = \langle d_{ia} d_{ib} \rangle$ and hence the nematic order parameter $Q_{ab} = \sum_i (P_{ab}^i - \delta_{ab} \sum_c P_{cc}^i/3)$ can be directly obtained in terms of the P_{ab}^i fields.

Consequently, we can now seek the saddle point solution to the above action. At the saddle point, the constraint fields are time-independent and the \mathbf{d}_i fields can be integrated out. Notice that in contrast to the clean system, the constraint fields λ_i are space-dependent. The mean-field action becomes

$$S_{\text{MF}} = \sum_i \text{Tr}[\ln G_{\text{MF}}^{-1}] - \int d\tau \left[\sum_i \left(i\lambda_i - i \sum_{ab} N_{ab}^i P_{ab}^i \right) + \nu \sum_{\langle ij \rangle} \sum_{abcd} P_{ac}^i \Gamma_{ij}^{abcd} P_{bd}^j \right] \quad (19)$$

$$G_{\text{MF}}^{-1}(\tau, \lambda_i, N^i) = [(-\partial_\tau^2 + i\lambda_i) \delta_{ab} - iN_{ab}^i] \quad (20)$$

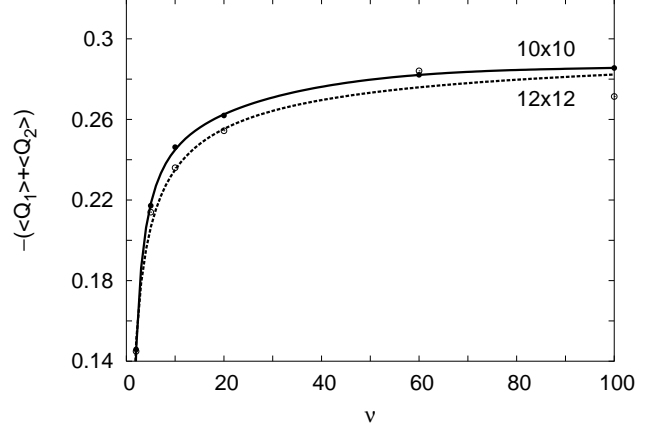


FIG. 2: $-(\bar{Q}_1 + \bar{Q}_2)$ as a function of $\nu = g/4U$ for $(\bar{\Lambda}^x - \bar{\Lambda}^z)/\delta\Lambda = 0.03$. This result, obtained for $N_S = 10 \times 10$ and $N_S = 12 \times 12$ lattices, shows that for a wide range of $\nu > \nu_c$ the ground-state remains biaxial nematic. [Note: $\bar{Q}_1 = \langle Q_1 \rangle$, $\bar{Q}_2 = \langle Q_2 \rangle$]

The saddle point equations can now be obtained from Eq. 19,

$$1 = \int \frac{d\omega}{2\pi} \sum_a [G_{aa}^{MF}(\omega, \lambda_i, N^i)] \quad (21)$$

$$iN_{ab}^i = \nu \sum_{cd} \sum_j \Gamma_{abcd}^{ij} P_{cd}^j \quad (22)$$

$$P_{ab}^i = \int \frac{d\omega}{2\pi} G_{ab}^{MF}(\omega, \lambda_i, N^i) \quad (23)$$

and are solved numerically to obtain the mean field order parameter $Q_{ab} = \sum_i (P_{ab}^i - \delta_{ab} \sum_c P_{cc}^i/3)$ for each disorder realization.

For a given disorder realization, we solve the set of mean-field equations Eqs. 21, 22, and 23 in order to find, for each lattice site i , the fields P_{ab}^i (with $a, b = \{x, y, z\}$). We then average over 100 disorder realizations and for finite sizes $N_S = 10 \times 10$ and 12×12 . We find that the real valued solutions of the order parameter are diagonal and obtain $\bar{Q}_a = \langle Q_a \rangle_{\text{disorder}} \equiv (-\langle \bar{Q}_1 + \bar{Q}_2 \rangle, \bar{Q}_1, \bar{Q}_2)$. The result is shown in Fig. 2 for $(\bar{\Lambda}^x - \bar{\Lambda}^z)/\delta\Lambda = 0.03$. We find, from the plot of $-(\bar{Q}_1 + \bar{Q}_2)$ as a function of ν , that the biaxial phase persists for a wide range of $\nu > \nu_c \equiv 1$. This shows that the effect of quantum fluctuations, at least at a saddle point level, does not destabilize the biaxial phase as long as $\nu > \nu_c$. This qualitative feature seems to be independent of system size, as can be seen from Fig. 2 and we expect it to hold in the $N_S \rightarrow \infty$ limit.

III. ULTRACOLD SPIN-ONE ATOMS

In this section we first show that the low energy effective Hamiltonian of spin-one ultracold atoms in the Mott insulating phase can be mapped onto the rotor Hamiltonian (Eq. 1) which we analyzed earlier. Then we propose an imaging experiment on ultracold atoms which can detect the biaxial nematic phase.

A. Effective rotor model

We consider a system of bosonic $S = 1$ atoms in a disordered optical lattice with spin-dependent confining potentials and antiferromagnetic interaction between atoms. The many-body Hamiltonian for this system is given in second-quantized notation by

$$\mathcal{H} = \int d\mathbf{r} \hat{\psi}_a^\dagger(\mathbf{r}) \left(-\frac{\hbar^2}{2m} \nabla^2 + V_a(\mathbf{r}) \right) \hat{\psi}_a(\mathbf{r}) + \frac{1}{2} \int d\mathbf{r} d\mathbf{r}' \hat{\psi}_a^\dagger(\mathbf{r}) \hat{\psi}_a^\dagger(\mathbf{r}') W(\mathbf{r} - \mathbf{r}') \hat{\psi}_b(\mathbf{r}') \hat{\psi}_b(\mathbf{r}), \quad (24)$$

where $\hat{\psi}_a^\dagger(\mathbf{r})$ is the boson field operator that creates a particle with spin projection $a = \{-1, 0, 1\}$ at position \mathbf{r} , $V_a(\mathbf{r})$ is the spin-dependent and spatially disordered external potential, and $W(\mathbf{r} - \mathbf{r}') = \delta(\mathbf{r} - \mathbf{r}') (U_0 + U_2 \mathbf{S}_1 \cdot \mathbf{S}_2)$ is the two-body interatomic potential¹⁸. Here $U_2 = \frac{4\pi\hbar^2}{3m} (a_2 - a_0)$ and $U_0 = \frac{4\pi\hbar^2}{3m} (2a_2 + a_0)$ are the on-site interactions, $a_{2(0)}$ are the s-wave scattering lengths in the $S = 2(0)$ spin channels, and m is the mass of the atoms. For example, for ²³Na, the scattering lengths are $a_2 = (52 \pm 5)a_B$ and $a_0 = (46 \pm 5)a_B$ where a_B is the Bohr radius¹² so that $U_2/U_0 \sim 0.04$. In what follows, we shall be interested in the Mott states of the spin-one bosons which occur in the limit of deep lattice potential with $V_1 = V_{-1} \neq V_0$.

A spin-dependent disordered potential $V_a(\mathbf{r})$ can be generated by superposing a speckled laser field on a sinusoidal spin-dependent lattice potential $V_{0a}(\mathbf{r})$. The spin dependence of the sinusoidal potential can be achieved by tuning the laser frequency close to the hyperfine splitting (but far away from the fine structure splitting) of the atoms^{19,20,21,22,23,24}. In appendix A, we propose a method to obtain a spin-dependent lattice potential with $V_1 = V_{-1} \neq V_0$. Generation of the disordered potential $\delta V_a(\mathbf{r})$ can be achieved by reflecting a laser at the same frequency but with a much lower intensity off a speckled mirror. The net lattice potential seen by the atoms at spin state a is then $V_a(\mathbf{r}) = V_{0a}(\mathbf{r}) + \delta V_a(\mathbf{r})$. In what follows, we shall consider the situation where the speckled field laser is weak compared to the one generating the sinusoidal potential such that $\delta V_a \ll V_{0a}$.

For free ultracold atoms in an optical lattice, the energy eigenstates are Bloch wave functions and a superposition of these Bloch states yields a set of Wannier functions which are well localized on the individual lattice sites for deep lattices²⁵. The energies involved in the system dynamics being small compared to excitation energies to the second band, we expand the boson field operators in the Wannier basis and keep only the lowest states, $\psi_a(\mathbf{r}) = \sum_i b_{ia} w(\mathbf{r} - \mathbf{r}_i)$. Consequently, the many-body Hamiltonian (24) reduces to¹¹

$$\mathcal{H} = \frac{U_0}{2} \sum_i \hat{n}_i (\hat{n}_i - 1) + \frac{U_2}{2} \sum_i (\mathbf{S}_i^2 - 2\hat{n}_i) - \mu \sum_i \hat{n}_i - \sum_{\langle ij \rangle} \sum_a \left(b_{ia}^\dagger \tilde{t}_a^{ij} b_{ja} + \text{h.c.} \right), \quad (25)$$

where b_{ia} is the spin-one boson operator at site i with spin projection $a = \{-1, 0, 1\}$, $\hat{n}_i = \sum_a b_{ia}^\dagger b_{ia}$ is the boson density at site i , $\hat{\mathbf{S}}_i = \sum_{ab} b_{ia}^\dagger \mathbf{S}_{ab} b_{ib}$ is the spin operator (\mathbf{S} being the spin rotation matrices for spin-one bosons), μ is the chemical potential, and \tilde{t}_a^{ij} are given by

$$\tilde{t}_a^{ij} = \int d\mathbf{r} w^*(\mathbf{r} - \mathbf{r}_i) \left(-\frac{\hbar^2}{2m} \nabla^2 + V_a(\mathbf{r}) \right) w(\mathbf{r} - \mathbf{r}_j). \quad (26)$$

so that $\tilde{t}_1 = \tilde{t}_{-1} \neq \tilde{t}_0$ for $V_1 = V_{-1} \neq V_0$.

Note that for weak speckled fields, we always have $\sigma_t/\bar{t}_a \ll 1$, where σ_t and \bar{t}_a are the standard deviation and average of the hopping coefficient \tilde{t}_a . However, in this setup, one can always tune the sinusoidal potential V_{0a} so that we are in a regime where $|\bar{t}_1 - \bar{t}_0|/\sigma_t \ll 1$. As we shall see, this is precisely the regime where one expects to see the biaxial phase. Also we note that due to the on-site disordered potential, the chemical potential μ_i should also be site-dependent. However, μ_i has only a power law dependence on disorder by comparison to an exponential dependence for the hopping coefficients. Consequently, the standard deviation of μ_i is small and does not influence the nature of the Mott states. So we replaced μ_i by its average value μ in Eq. 25. Notice that this approximation is valid only when the potential due to the speckled field is weak compared to the one due to the sinusoidal field.

Next, following Ref. 12, we switch to a representation where the boson operators transform as vectors under spin rotation

$$b_{iz} = b_{i0}, \quad b_{ix} = \frac{1}{\sqrt{2}}(b_{i-1} - b_{i1}), \quad b_{iy} = \frac{-i}{\sqrt{2}}(b_{i-1} + b_{i1}). \quad (27)$$

Using these operators, the kinetic term in (25) is rewritten as

$$- \sum_{\langle ij \rangle} \sum_{a \in \{x,y,z\}} \left(b_{ia}^\dagger t_a^{ij} b_{ja} + \text{h.c.} \right), \quad (28)$$

with $t_x^{ij} = t_y^{ij} = 2\tilde{t}_1^{ij}$ and $t_z^{ij} = \tilde{t}_0^{ij}$.

We now consider this spin-one Bose-Hubbard model in the limit where $N \gg 1$ and we are in the Mott phase of the bosons with a large odd number (N) bosons per site. A straightforward generalization of the analysis of Ref. 12, shows that the low energy effective Hamiltonian in this limit can be mapped on to a rotor model. Using the decomposition $b_{ia} = d_{ia} a_i$, where the boson operator a_i changes the number of particles N_i but not the orientation of the boson spin given by \mathbf{d}_i , we obtain in second order perturbation theory^{11,12}

$$\mathcal{H}_{\text{eff}} = \frac{U_2}{2} \sum_i S_i^2 - \frac{2N^2 \bar{t}_x^2}{U_0} \sum_{\langle ij \rangle} \left(\sum_{a=x,y,z} d_{ia} \frac{t_a^{ij}}{\bar{t}_x} d_{ja} \right)^2. \quad (29)$$

Eq. 29 has to be supplemented with the constraint $N_i + S_i = \text{even}$ where N_i is the number of bosons at site i , and $S_i = i\epsilon_{ijk} d_j \frac{\partial}{\partial d_k}$ is the total spin which can be identified as the rotor angular momentum. However, the constraint $N_i + S_i = \text{even}$

becomes irrelevant in the small U_2 limit¹². Therefore in this limit, the effective low energy Hamiltonian (Eq. 29) can be directly mapped to the rotor model (Eq. 1) with the identification $U_2/2 \rightarrow U$, $2N^2\bar{t}_x^2/U_0 \rightarrow g$ and $t_a^{ij}/\bar{t}_x \rightarrow \Lambda_a^{ij}$. For the biaxial nematic phase to occur, we therefore need a window where the conditions $4N^2\bar{t}_x^2/U_2U_0 \gg 1$, and $N\bar{t}_x/U_0 < 1$ are simultaneously satisfied. The second condition arises here since we need to be away from the superfluid transition point of boson systems. These conditions can be expected to be easily satisfied. For example, in a deep lattice ($V = 10E_R$ where E_R is the recoil energy) set by red detuned light ($\lambda = 985$ nm) and containing about 10 sodium atoms per well, $4N^2\bar{t}_x^2/U_2U_0 \sim 14$, and $N\bar{t}_x/U_0 \sim 0.4$.

B. Detection of biaxial nematic order

In this section, we propose a method to detect experimentally biaxial nematic order in a condensate of spin-one cold atoms. Consider the atoms being in a Mott state which has biaxial nematic order parameter. First, as is customary in most of the experiments in ultracold atoms²⁵, we switch off both the lattice potential and the trap, and let the atoms expand freely. We then probe the expanding cloud by a right-circular (σ_+) polarized laser beam. The dielectric tensor of the atoms as seen by the laser beam is given by²³

$$\langle \epsilon_{jk} \rangle = \delta_{jk} + c_0 \langle \rho \rangle \delta_{jk} - ic_1 \epsilon_{jkl} \langle S_l \rangle + c_2 \langle Q_{jk} \rangle, \quad (30)$$

where the coefficients $c_{a=\{0,1,2\}}$ depends on the laser frequency and $\langle \rho \rangle$, $\langle \mathbf{S} \rangle$ and $\langle Q_{jk} \rangle$ are the density, average spin and the nematic order parameters of the atomic cloud. If the laser frequency is too far detuned from hyperfine splitting frequency of the atomic levels, c_2 vanishes and the nematic order is not probed. On the other hand, if the laser frequency is not detuned enough from the hyperfine splitting frequency, there will be significant absorption which will weaken the intensity of the transmitted light. As shown in Ref. 23, there indeed exist a window for several spin-one atom species where the imaging can be done.

If the expanding cloud is sufficiently optically thin and homogeneous, the polarization of the transmitted beam (taken to be propagating along the z axis) is

$$\varphi_{\text{out}} = e^{\frac{i\omega\Delta}{c}} \left[\mathbf{1} + \frac{i\omega}{c} \int_0^\Delta dz (\sqrt{\epsilon_{(xy)}} - \mathbf{1}) \right] \varphi_{\text{in}}, \quad (31)$$

where $\varphi_{\text{in}} = (\varphi_x, \varphi_y)$ is the two-component polarization vector of the incoming laser beam, $\epsilon_{(xy)}$ is the reduced dielectric tensor in the (xy) plane and Δ is the thickness of the medium. As discussed in Ref. 23, the presence of spin order $\langle \mathbf{S} \rangle$ in the atom cloud gives a phase shift to the atoms whereas a nematic order leads to a left-circular (σ_-) polarized component in the transmitted beam. So, if we shine on the spin-one sample a beam of pure σ_+ light in such a way that the principal axes Q_1 and Q_2 of the nematicity ellipsoid are orthogonal to the direction of the propagating beam, the intensity of the σ_- component of the transmitted beam is given by

$$I_- = |\alpha_+ \frac{i\omega c_2}{4c} \int_0^\Delta dz (\langle Q_1 \rangle - \langle Q_2 \rangle)|^2 \quad (32)$$

where α_+ is the amplitude of the incoming beam. Note that this method distinguishes between uniaxial and biaxial nematic ground states. In the uniaxial state $\langle Q_1 \rangle = \langle Q_2 \rangle$ and $I_- = 0$; however, for a biaxial nematic ground state $\langle Q_1 \rangle \neq \langle Q_2 \rangle$ so $I_- \neq 0$. Thus passing the transmitted beam through a crossed polarizer, one should be able to measure I_- and hence detect the presence of a biaxial nematic state.

IV. CONCLUSION

We have studied a disordered O(2) rotor model with quadrupolar interaction and demonstrated that the model exhibits a biaxial nematic phase in the disordered average sense. It is demonstrated that within mean-field analysis, the biaxial nematic phase is stable against small quantum fluctuations. Such models are shown to be realized in the Mott phase of spin-one ultracold bosons in optical lattices with spin-dependent disordered potential in the limit of large number of bosons per site. We have also suggested an experiment which can, using laser imaging of the spin-one atoms, detect the biaxial nematic phase.

Acknowledgments

This work was supported by NSERC, the Canadian Institute for Advanced Research, the Canada Research Chair Program (YBK, KS, JSB), and Le Fonds québécois de la recherche sur la nature et les technologies (JSB). YBK thanks Chetan Nayak for discussions that sparked his interest in biaxial nematic phases, KS thanks Duncan O'dell and Ying-Jer Kao for helpful discussions.

APPENDIX A: SPIN-DEPENDENT OPTICAL LATTICE

We propose here a method to create a spin-dependent optical square lattice. Using our approach, trapped bosons with $S_z = \{-1, 1\}$ experience the same potential, $V_{-1} = V_1$, while bosons with $S_z = 0$ are subject to a different potential V_0 .

Consider atoms with total angular momentum $S = 1$ interacting with a configuration of laser beams producing an electric field $\mathbf{E}(\mathbf{r})$. Building on previous work for $S = 1/2$ particles²⁴, we deduce that atoms with $S = 1$ experience an external potential of the form

$$V_{\alpha\beta}(\mathbf{r}) = V(\mathbf{r})\delta_{\alpha\beta} + \mathbf{B}(\mathbf{r}) \cdot \hat{\mathbf{S}}_{\alpha\beta} + N_{ij}(\mathbf{r})\hat{G}_{ij\alpha\beta}, \quad (\text{A1})$$

with $\alpha, \beta = \{-1, 0, 1\}$. In Eq. A1, the scalar potential $V(\mathbf{r})$ is proportional to the light intensity, the vector field $\mathbf{B}(\mathbf{r})$ is proportional to the electromagnetic spin²⁴ and couples to the total atomic angular momentum operator $\hat{\mathbf{S}}$, and the second-rank tensor $N_{ij}(\mathbf{r})$ is proportional to the light nematicity²³ and

couples to the quadrupole moment operator \hat{G}_{ij} :

$$\begin{aligned}
V(\mathbf{r}) &= b_0 \mathbf{E}^*(\mathbf{r}) \cdot \mathbf{E}(\mathbf{r}) \\
\mathbf{B}(\mathbf{r}) &= -ib_1 \mathbf{E}^*(\mathbf{r}) \times \mathbf{E}(\mathbf{r}) \\
N_{ij}(\mathbf{r}) &= b_2 \left[\frac{1}{2} (E_i^*(\mathbf{r}) E_j(\mathbf{r}) + E_j^*(\mathbf{r}) E_i(\mathbf{r})) \right. \\
&\quad \left. - \frac{1}{3} \mathbf{E}^*(\mathbf{r}) \cdot \mathbf{E}(\mathbf{r}) \delta_{ij} \right] \\
\hat{\mathbf{S}}_{\alpha\beta} &= \langle 1, \alpha | \hat{\mathbf{S}} | 1, \beta \rangle \\
\hat{G}_{ij\alpha\beta} &= \langle 1, \alpha | \left[\frac{1}{2} (\hat{S}_i^\dagger \hat{S}_j + \hat{S}_j^\dagger \hat{S}_i) - \frac{1}{3} \hat{\mathbf{S}}^2 \delta_{ij} \right] | 1, \beta \rangle.
\end{aligned} \tag{A2}$$

The coefficients $b_{0,1,2}$ are functions of the light frequency and the atomic structure. To obtain an effective coupling to the light nematicity (i.e. a large enough b_2 value), one needs to tune the laser frequency close to the hyperfine splitting of the atoms, but far from the fine structure splitting such that $b_1 \ll b_2, b_0$.

Then, to generate the optical square lattice (say in the xy plane), we use two orthogonal pairs of counter propagating monochromatic lasers, and choose these equal intensity light fields to be linearly polarized in the z direction. The total electric field produced by this configuration is thus given by

$$\mathbf{E}(t, x, y) = 2 E_0 \hat{\mathbf{z}} e^{i\omega t} \left[e^{i\phi_x} \cos(kx) + e^{i\phi_y} \cos(ky) \right], \tag{A3}$$

where k is the wavevector, and ϕ_x, ϕ_y are the initial phases for the electric field propagating in the x and y directions respectively. We choose the difference between these two initial phases $\Delta\phi = \phi_x - \phi_y$ to be equal to $\pi/2$. Using this electric field configuration, we find the electromagnetic spin to be zero and the external potential to be

$$\begin{aligned}
V_{\alpha\beta}(x, y) &= 4|E_0|^2 (\cos^2(kx) + \cos^2(ky)) \times \\
&\quad \left((b_0 - \frac{2}{3}b_2) \delta_{\alpha\beta} + b_2 \langle 1, \alpha | \hat{S}_z^2 | 1, \beta \rangle \right).
\end{aligned} \tag{A4}$$

Hence, only the diagonal terms of the external potential tensor are non-zero and are given by

$$\begin{aligned}
V_{00} &= A(x, y) (b_0 - \frac{2}{3}b_2) \\
V_{11} &= A(x, y) (b_0 + \frac{1}{3}b_2) \\
V_{-1-1} &= A(x, y) (b_0 + \frac{1}{3}b_2),
\end{aligned} \tag{A5}$$

where $A(x, y) = 4|E_0|^2 (\cos^2(kx) + \cos^2(ky))$. As a result, we obtain a spin-dependent optical square lattice with $V_1 = V_{-1} \neq V_0$.

¹ See chapter 2 in P.G. de Gennes and J. Prost *The Physics of Liquid Crystals* (Oxford University Press, New York, 1993).
² K. Merkel *et al.*, Phys. Rev. Lett. **93**, 237801 (2004).
³ For a review on defect structures of biaxial nematic see N.D. Mermin, Rev. Mod. Phys. **51** 591 (1979).
⁴ C.J. Halboth and W. Metzner, Phys. Rev. Lett. **85**, 5162 (2000).
⁵ V. Oganesyan, S.A. Kivelson, and E. Fradkin, Phys. Rev. B **64**, 195109 (2001).
⁶ H.Y. Kee and Y.B. Kim, Phys. Rev. B **71**, 184402 (2005).
⁷ S.A. Kivelson, I.P. Bindloss, E. Fradkin, V. Oganesyan, J.M. Tranquanda, A. Kapitulnik and C. Howald, Rev. Mod. Phys. **75**, 1201 (2003).
⁸ A.F. Andreev and I.A. Grishchuk, Sov. Phys. JETP **60**, 267 (1984).
⁹ P. Chandra and P. Coleman, Phys. Rev. Lett. **66**, 100 (1991).
¹⁰ L.P. Gor'kov and A. Sokol, Phys. Rev. Lett. **69**, 2586 (1992).
¹¹ E. Demler and F. Zhou, Phys. Rev. Lett. **88**, 163001 (2002).
¹² A. Imambekov, M. Lukin, and E. Demler, Phys. Rev. A **68**, 063602 (2003).
¹³ F. Zhou and M. Snoek, Ann. Phys. **308**, 692 (2003).
¹⁴ P. Horak, J.Y. Courtois, and G. Grynberg, Phys. Rev. A. **58**, 3953 (1998).
¹⁵ J.E. Lye, L. Fallani, M. Modugno, D. Wiersma, C. Fort, and M.

Inguscio, Phys. Rev. Lett. **95**, 070401 (2005).
¹⁶ In the case of $N_S = 20 \times 20$, we have studied four different systems sizes starting from 20×8 up to 20×14 , and extrapolated the order parameter to its 20×20 value.
¹⁷ H. Kleinert *Path Integrals in Quantum Mechanics, Statistics, Polymer Physics and Financial Markets* (World Scientific, Singapore, 2004).
¹⁸ C.J. Pethick and H. Smith *Bose-Einstein Condensation in Dilute Gases* (Cambridge University Press, Cambridge, 2002).
¹⁹ D. Jaksch, H. Briegel, J. Cirac, C. Gardiner, and P. Zoller, Phys. Rev. Lett. **82**, 1975 (1999).
²⁰ G. Brennen, C. Caves, P. Jessen, and I. Deutsch, Phys. Rev. Lett. **82**, 1060 (1999).
²¹ W.V. Liu, F. Wilczek, P. Zoller, Phys. Rev. A **70**, 033603 (2004).
²² O. Mandel, M. Greiner, A. Widera, T. Rom, T. Hänsch, and I. Bloch, Phys. Rev. Lett. **91**, 010407-1 (2003).
²³ I. Carusotto and E. Mueller, J. Phys. B **37**, S115 (2004).
²⁴ A. Duradev, R.B. Diener, I. Carusotto, and Q. Niu, Phys. Rev. Lett. **92**, 153005-1 (2004).
²⁵ M. Greiner, O. Mandel, T. Esslinger, T.W. Hänsch, and I. Bloch, Nature **415**, 39 (2002); D. Jaksch, C. Bruder, J.I. Cirac, C.W. Gardiner, and P. Zoller, Phys. Rev. Lett. **81**, 3108 (1998).